



THE UNIVERSITY *of* EDINBURGH

Edinburgh Research Explorer

Joint exploitation of wave and offshore wind power

Citation for published version:

Cradden, L, Mouslim, H, Duperray, O & Ingram, D 2011, Joint exploitation of wave and offshore wind power. in *EWTEC 2011 Proceedings*.

Link:

[Link to publication record in Edinburgh Research Explorer](#)

Document Version:

Peer reviewed version

Published In:

EWTEC 2011 Proceedings

General rights

Copyright for the publications made accessible via the Edinburgh Research Explorer is retained by the author(s) and / or other copyright owners and it is a condition of accessing these publications that users recognise and abide by the legal requirements associated with these rights.

Take down policy

The University of Edinburgh has made every reasonable effort to ensure that Edinburgh Research Explorer content complies with UK legislation. If you believe that the public display of this file breaches copyright please contact openaccess@ed.ac.uk providing details, and we will remove access to the work immediately and investigate your claim.



Joint Exploitation of Wave and Offshore Wind Power

Lucy Cradden^{#1}, Hakim Mouslim^{*2}, Olivier Duperray⁺³, David Ingram^{#4}

[#]*Institute for Energy Systems, University of Edinburgh
Kings Buildings, Edinburgh EH9 3JL, United Kingdom*

¹lucy.cradden@ed.ac.uk

⁴david.ingram@ed.ac.uk

^{*}*Ecole Centrale de Nantes*

1 rue de la Noë, BP 92101, 44115 Nantes Cedex 3

²hakim.mouslim@ec-nantes.fr

⁺*Tecnalia*

Parque Tecnológico de Bizkaia, C/ Geldo, Edificio 700, 48160 Derio, Spain

³olivier.duperray@tecnalia.com

Abstract—This paper presents some preliminary analysis of three European marine energy test sites in terms of their potential suitability for deployment of renewable energy platforms combining more than one technology. An understanding of the resources and their correlation in time is developed, followed by an analysis of the different power production characteristics from some hypothetical combinations of wind and wave energy devices. Finally, a case study is presented, demonstrating how the addition of wave power to an offshore wind site could offer some advantages in relation to meeting consumer demand.

Keywords— Wave, offshore wind, combined platforms, correlation, demand.

I. INTRODUCTION

This work is being carried out as part of the MARINA Platform FP7 project (Grant agreement number: 241402), the main theme of which is the investigation of the potential for combined technology marine renewable energy platforms (MREs). The project aims to produce evaluation criteria, design and optimisation tools, and preliminary engineering designs for some MREs utilising more than one renewable energy technology [1]. Two of the key outputs to which this particular study relates are the development of a protocol for combined wind, wave and current resource analysis, and a spatial decision support tool for combined technology platforms. Both these tasks aim to assist in the identification of sites that would be suitable for installation of a combined technology platform, and indeed where a combined technology platform could be more advantageous than a single technology. This paper is concerned, in particular, with the possible co-location of wind and wave energy devices.

There are a number of likely benefits to combining different renewable energy technologies at a single site, particularly in deep water. As the offshore wind industry grows and the technology advances, it is becoming more feasible to develop sites in regions of deeper water, for example, using floating wind turbines. However, this infant technology is costly, and there is a strong need to reduce these costs in order to push development further. Installation and maintenance costs at deep water sites are also prohibitive. It is

known that there are sites in European waters with extensive wave energy resources, so combining offshore wind technology with wave energy converters (WECs) on a single platform could increase the site utilisation factors (i.e. the amount of power per square metre), whilst reducing the capital, installation and maintenance costs, and thus the cost per unit of energy produced. Additionally, by installing wave energy devices, which are at an earlier stage of development than wind turbines, combined platforms can be used to ‘pull’ wave technology and provide a base for long-term, large-scale development whilst relying on the consistent performance expected from wind devices.

The specific aspect of combined technologies being explored in this study is the differing characteristics of the energy production from wind and wave devices. For co-located wind and wave energy devices, the potential to reduce power output variability could be a particular advantage. More consistent output is always desirable - it would have consequent benefits for the electricity network, and output which is strongly correlated with peak consumer demand levels would be particularly beneficial.

The ability to deliver a less variable power output from a platform utilising both wind and wave devices depends strongly on the correlation between the two resources at individual sites. Having wind and wave resources at a site that are generally uncorrelated would reduce the likelihood that peaks and troughs in both resources would occur simultaneously. A potentially exploitable aspect of offshore renewable resources is that, in locations that tend to have high wind speeds and also a long fetch, the wave resource may follow the wind resource with a distinct time delay, so that they show low correlations at time zero and maximum correlation at a given time lag. A consistent lag between peaks in wind and wave power could mean that, when combined, the overall resource is ‘smoother’.

The relationship between wind and wave energy resources at three existing European marine energy test sites is examined in this paper in terms of raw power availability. The consequent power characteristics of hypothetical

combinations of wave and wind energy devices are investigated with a view to establishing some optimum combinations at each site. Finally, a preliminary case study analysing production with respect to consumer demand, and the potential advantage of inclusion of wave power over a site utilising solely wind generation is presented.

II. BI-VARIATE WIND-WAVE DATA SITE DESCRIPTIONS

A. Methodology

In order to establish correlation between wind and wave power, instrumental site measurements and/or outputs from numerical models are required. The offshore wind sector in Europe has only a few references for simultaneous wave and wind data collection, for example, in [2].

In the case of wave energy applications, offshore measurements are common, but it is important to note that highly energetic sites require robust instrumentation platforms. Non-intrusive measurements exist, such as satellite datasets, which enable long term data collection. However, these have typically low temporal resolution and limited spatial resolution [3]. Up to date, floating wave-rider buoy measurements provide the most reliable data containing directional, spectral sea-state descriptions. Such measurements are very reliable but do require continuous buoy operation and maintenance, and thus tend to be deployed for short periods only, making them unsuitable for long-term wave climate characterization.

Offshore wind measurements are less readily available as physical on-site mast installations remain very costly. Numerical flow modelling enables the estimation of offshore wind climates from onshore coastal measurements when the distances remain acceptable. The numerical models can be calibrated using offshore satellite or floating buoy measurements.

For the present study, three European wave test sites were considered and each provided wave and wind directional data. There was an initial stage of data processing and quality-control. Uni-variate wind and wave climate descriptions describe each site and provide average power information. Bi-variate power correlations are examined and time-lag cross-correlation information is extracted from the time series for the three sites.

B. Locations and available data

Table 1 and Table 2 provide information about the data sources used for the analysis at each of the three sites. EMEC is the only test site with nearly 2 years of uninterrupted buoy data. For the remaining sites, complementary high-resolution models (the third generation wave spectral propagation models WAM (the WAMDI group, 1988 [4]) and Previmer (SHOM Loire model [5])) have been used in the absence of long duration measurements. Comparisons have been made with wave buoy time series to assess the data robustness in these cases. The wind model, WRF (Weather Research and Forecast model, [6]) provided high resolution wind data, again where local measurements were unsuitable.

TABLE 1 WAVE DATA SOURCE DETAILS.

Wave data information	bimep	EMEC	SEM-REV
Longitude	2° 52.8'W	3° 34.7'W	2°47.2' W
Latitude	43° 27.6'N	58° 97.3'N	47°14.3' N
Available hours	17518	16868	10617
Data source	WAM model	Wave buoy	Previmer model
Model resolution	1.6 km	---	0.370 km
Depth	80 m	~50 m	35 m

TABLE 2 WIND DATA SOURCE DETAILS.

Wind data information	bimep	EMEC	SEM-REV
Longitude	2° 52.8'W	3° 34.7' W	3°13.2' W
Latitude	43° 27.6'N	58° 97.3' N	47°18.1' N
Available hours	17518	16868	17518
Data source	WRF model	WRF model	Met mast
Model resolution	12 km	5km	---
Met mast altitude	10 m	10 m	34 m

C. Model and wave buoy data reanalysis

Two wave models have been used in the cases of the bimep [7] and SEM-REV test sites. The wave models' accuracies have been estimated using scatter plots and show good correlation with the existing measured wave data for an overlapping time period. Fig. 1 presents the scatter plots for a number of hourly samples which were provided for the bimep site.

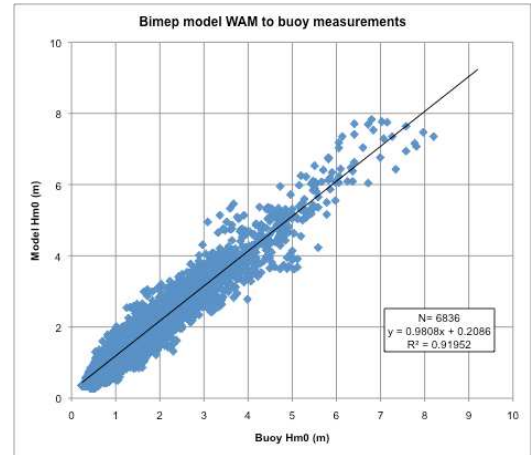


Fig. 1 Data accuracy verification. The plot shows the bimep significant wave height Hm0 from model WAM against buoy measurements of Hm0.

The calculated significant wave height correlation coefficient reaches values of $\gamma = 0.96$ ($R^2 = 0.92$) for bimep and $\gamma = 0.92$ ($R^2 = 0.85$) for SEM-REV, for $N=6836$ and 8758 samples respectively. In the rest of the study, it is therefore assumed that the wave models used for SEM-REV and bimep have sufficiently good accuracy and reflect the wave climatology of each site. It is, however, noted that these models show weaker correlation for other factors, such as direction or peak period as in [7].

D. Bivariate climate description

The available power resource is computed using wave and wind potential linear theory. Wave power density, P_{wave} is dependent on spectral zero-order wave height, H_{m0} ,

$$H_{m0} = 4\sqrt{m_0} \quad (1)$$

and the energy period, T_e ,

$$T_e = \frac{m_1}{m_0} \quad (2)$$

where m_0 and m_1 are the zeroth and first moments of the spectrum respectively. P_{wave} is defined by:

$$P_{wave} = \frac{\rho_{water} g^2 H_{m0}^2 T_e}{32\pi} \left[\frac{W}{m} \right] \quad (3)$$

where ρ_{wave} is the water density, and g the gravitational acceleration.

Wind power is dependent only on the velocity, v . The power density per unit area, P_{wind} , is quantified using the formulation:

$$P_{wind} = \frac{1}{2} \rho_{air} v^3 \left[\frac{W}{m^2} \right] \quad (4)$$

where ρ_{air} is air density.

The available powers calculated from (3) and (4) for each site are shown in Table 3. Bi-variate correlation between sea state wave power and area wind power is found through computation of the joint occurrence probability of the two variables. The joint probability density function is defined as the product of the marginal and conditional probability density functions:

$$f_{X,Y}(x, y) = f_{X|Y}(y | x) f_X(x) = f_{Y|X}(x | y) f_Y(y) \quad (5)$$

The joint distribution is constrained by the probability integral condition:

$$\int_x \int_y f_{X,Y}(x, y) dy dx = 1 \quad (6)$$

TABLE 3 UNI-VARIATE WAVE AND WIND POWER SITE DESCRIPTION

	bimep	EMEC	SEM-REV
Mean wind power	0.214 kW/m ²	0.372 kW/m ²	0.260 kW/m ²
Mean wave power	26 kW/m	29 kW/m	14 kW/m
Max probability density	0.0280	0.4283	0.0703

Wind and wave joint distribution is obtained by fitting wind power to a Rayleigh marginal distribution. The joint probability densities shown in Fig. 2 describe simultaneous wind and wave power conditions and assess their probability of occurrence. The dependency level between the two variables is readable from the bi-variate distribution. This joint occurrence probability is fast to compute and is based on a simple statistical model. Other statistical models have been shown by Nerzic et al. [8] using the Plackett theory but require two independent marginal distributions.

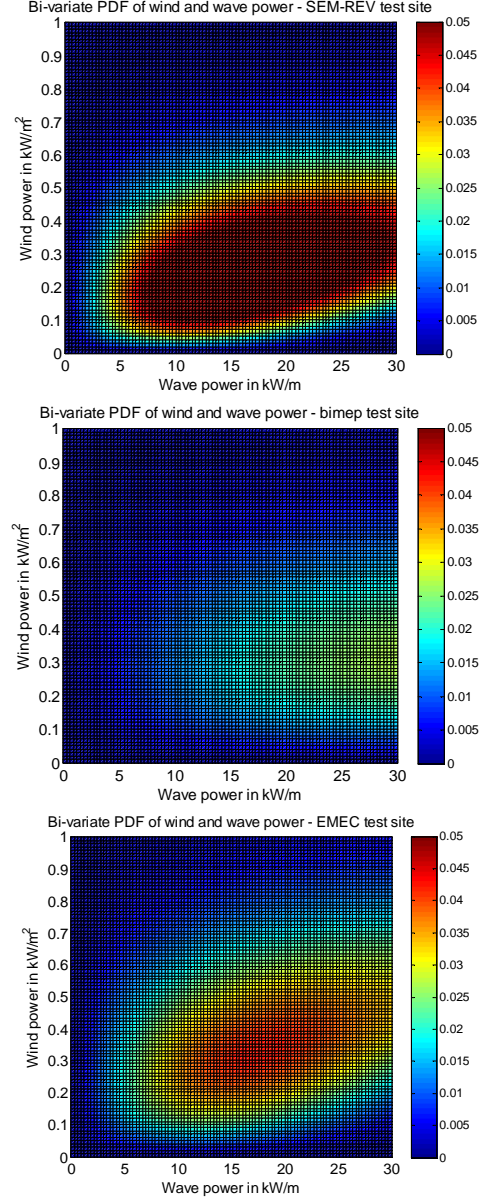


Fig. 2 Joint distribution plots for the three test sites using fitted Rayleigh marginal distributions.

For bimep and SEM-REV, the results in Fig. 2 show that the mean powers correspond to the peak of correlation. At EMEC, the mean wave power falls just outside the peak. The bi-variate probability is governed by the conditional distribution of wind over waves. EMEC has the narrowest correlation band between wave and wind power. The EMEC joint distribution suggests high probability of high wind speeds in presence of highly energetic sea states. On the other hand, SEM-REV has the widest joint distribution spread. This confirms a low correlation of wind and wave power on this test site. Finally, the bimep test site shows a lack of correlation for the low energetic seas and a high concentrated correlation over highly powerful sea-states.

E. Wave and wind time lag cross-correlation

Temporal cross-correlation between wind and wave is quantified in Fusco & al. [9], where the covariance formulation for two discrete variables is used. The cross-correlation is a function of a time lag between wind and wave power, which reflects the temporal relationship between the two variables. Equation 7 is the general formula for calculating the correlation, c , as a function of the time lag, τ , between two variables, x and y , at a point in time, k

$$c(\tau) = \frac{1}{N} \sum_{k=1}^{N-\tau} \frac{[x(k) - \mu_x][y(k+\tau) - \mu_y]}{\sigma_x \sigma_y} \quad (7)$$

where N is the number of samples, μ_x and μ_y are the sample means and σ_x and σ_y the standard deviations. Values between -1 and 1 describe the level of correlation between the two time series. At the origin, $C(0) = 0$ implies no correlation between wind and wave power; $C(0) = + / - 1$ describes a strong correlation.

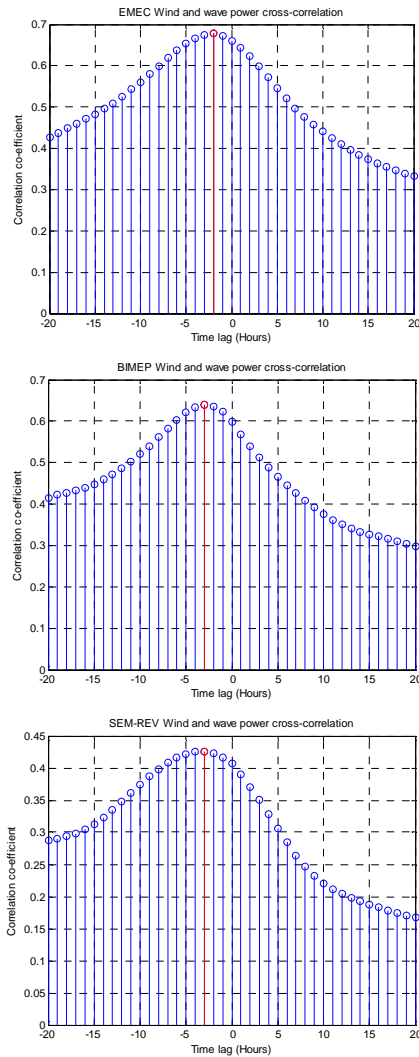


Fig. 3 Temporal cross-correlation for wind and wave power at the three test sites.

The temporal cross-correlations in Fig. 3 show a maximum correlation between the wind and wave power in the 0.4-0.7

range for the three sites. This leads to the conclusion that wind and wave power have medium to high correlation for the three test sites. The correlation coefficient values show good agreement with the joint distribution plots. The widest distribution corresponds to a low cross-correlation value which is the case for SEM-REV. Bimep and EMEC have a high correlation value in agreement with the bi-variate distribution shape. Finally, the time lag shows that for the three sites, wind is present before waves, with the highest correlation values at lags of 1-5 hours. As time advances, the correlation falls. In the case of SEM-REV, the correlation coefficient decreases rapidly with positive time lags.

III. WIND/WAVE AGGREGATE POWER PRODUCTION

A. Power production from wind and waves

Following the analysis of available offshore wind and wave resources and their levels of correlation, this part of the study intends to characterise the power production from a mix of wave energy converters and wind turbines in order to assess the potential benefits of combining both sources of power.

While comparing the power production figures from wind and wave, it is important to bear in mind that these two renewable energies are at a very different stage of development. The wind energy industry already has a proven track record of successful commercial deployment over nearly two decades, while the wave energy stakeholders still have to prove the commercial viability of their devices. Regarding this study, this means that the estimation of wave power production carries a level of uncertainty far greater than that of wind energy.

B. Power production of combined wind-wave energy

The wind energy outputs detailed in this document were calculated from the turbine power curve of the Vestas V90 3MW [10], a common turbine for both onshore and offshore wind parks. Wind velocities at 80m were used to derive hourly power outputs (the wind is extrapolated from 10m wind velocities to an altitude of 80m assuming a log profile law with a roughness coefficient of 0.0003m), assuming a full operation of the turbine over the whole duration for each site.

Due to the wide range of Wave Energy Converters (WECs) in development, an assessment of various devices was done initially to select a device suitable for all sites. The WECs assessed in this study were the Pelamis [11], a heaving self-reacting two-body device (as described in [12]) and the Wave Dragon [13]. The produced power was obtained from the power matrix of each device for the bin (wave height, wave period) corresponding to the hourly wave conditions measured at the 3 testing sites. Although the uncertainty around this method is quite high as parameters such as wave direction or sea state spectral bandwidth are not taken into account, it is considered relevant at this conceptual level to provide qualitative information and compare the evolution of energy production from various mixes of wave and wind energy. Finally, the Pelamis was selected for the following wave energy power calculations, as it was the most well-adapted WEC for all sites (with results close to Wave Dragon).

The power production has been calculated for approximately 2 years at each test site for a mix of wind and wave energy, according to the following scenarios: 100% Wind; 75:25 Wind-Wave; 50:50 Wind-Wave; 25:75 Wind-Wave; and 100% Wave. Fig. 4 shows the power production calculated at bimep for a sample of 25 days (600hours). The graph produced for bimep highlights periods when power production from waves is higher than wind production (orange) and periods when wind power production is predominant (green). Due to the high efficiency of today's wind turbine, we can observe that each wind event leads to the optimal operation of the wind turbine, often reaching rated power. Significant sea states, which contain far more energy to be potentially extracted, are less well exploited by WECs. In the case of bimep we can observe the occurrence of a swell clearly independent from the wind, an event common at this site due to an average wind energy resource and a rather good wave energy resource characterised by the occurrence of long swells originating from the North Atlantic.

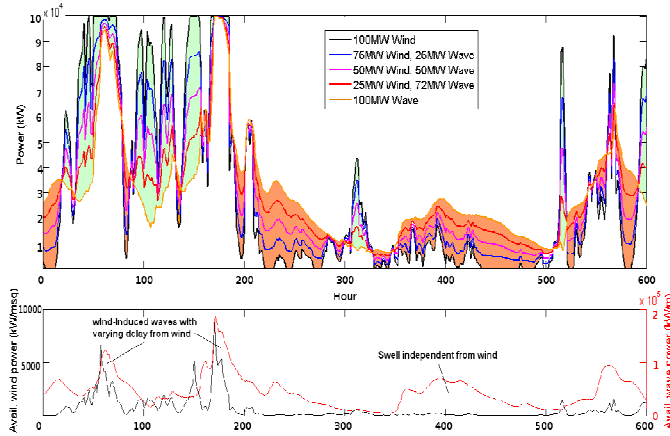


Fig. 4 25 days of wind/wave energy mix at bimep

The main parameters for both wind and wave energy are detailed in Table 4. As expected, the capacity factors (ratio of produced power over nominal rated power over the total duration) for wind energy far exceed those for wave energy. These values vary from site to site. The bimep site offers less potential for wind energy due to a rather low resource (a different wind turbine would possibly be more suitable for this site). At EMEC and SEM-REV, the wind resource is more favourable with a higher wind velocity and lower standard deviation.

At bimep, introducing wave energy to an offshore wind farm would significantly decrease the number of hours of zero power output, from a maximum for 100% wind of 17.5% of the time (approx. 1500 hrs per year) down to 8.7% with 100% wave (approx. 750 hrs per year).

At EMEC, the scenarios with 100% wind and 100% wave present a zero power output for respectively 7.6% and 11.8% of the total time. The latter value is slightly higher than at bimep, probably due to wave conditions that are outside the operational conditions of the WECs (more storm events, for example, when WECs don't generate electricity). It becomes

very interesting to mix both sources of energy as zero power outputs reduce to 1.2% of the time.

At SEM-REV, the ideal situation is for a combination of wave and wind energy, when no power is produced only 2.4% of the time. For wind only, no power is produced for 6.9% of the time, while a wave energy only scenario would be characterised by numerous periods of no power output – 32% of the time. On the other hand, periods of operation at nominal power (100MW) generally decrease for the three locations as wave energy is introduced due to the higher efficiency of wind energy turbines.

TABLE 4 WAVE AND WIND ENERGY MAIN PARAMETERS

	bimep		EMEC		SemRev	
100% of:	Wind	Wave	Wind	Wave	Wind	Wave
Available power (wind: kW/m ² – wave: kW/m)						
Mean	0.52	26	0.81	30	0.54	14
Deviation	1.13	42	1.07	51	0.81	31
Produced power						
Capacity Factor	24.1	17.5	40.3	22.4	34.3	9.5
% of time no power	17.5	8.7	7.6	11.8	6.9	32.0
% of time full power	6.2	0.3	10.8	1.8	5.7	0.07

Fig. 5, Fig. 6, and Fig. 7 summarise the non-exceedance distribution of power production levels for the 3 sites. At bimep, the wind resource is not very high and, in spite of the low level of development of WECs, a 100% wave scenario would have higher power outputs than 100% wind during slightly more than 60% of the time. This graph also clearly shows that introducing wave energy to the mix affects the number of hours operating at rated power but also decreases the duration of no power output. Comparing the green and magenta curves, we can note that a 100% wave scenario has globally the same outputs as a 25% wind / 75% wave, but this latter would be preferred as being always slightly higher in terms of produced power and, more importantly, decreasing the periods of no power from 8.7% to 1.6%. Overall, a 50% wind / 50% wave scenario seems to be the most suitable mix for bimep.

At EMEC, the tendencies shown in Fig. 6 are quite different. This can be explained mainly by the higher wind regime. For 60% of the time a 100% wind scenario would provide higher power outputs. For energy levels less than 20MW (20% of rated capacity), introducing wave energy helps to decrease the number of hours of zero power from 7.6% for wind only down to 1.2% for a mix of wave and wind. At this site, we can anticipate that in the coming years more optimized WECs would be able to efficiently capture the high wave energy resource available, leading to a higher ratio of wave energy in the wind / wave mix. Finally, we can expect the scenario 75% wind / 25% wave, represented by the red curve on the graph, to be most adequate for EMEC. The behaviour is quite close to the 100% wind and, although there is a slight loss of hours

at rated power, the production is higher for 40% of the time at lower levels of power.

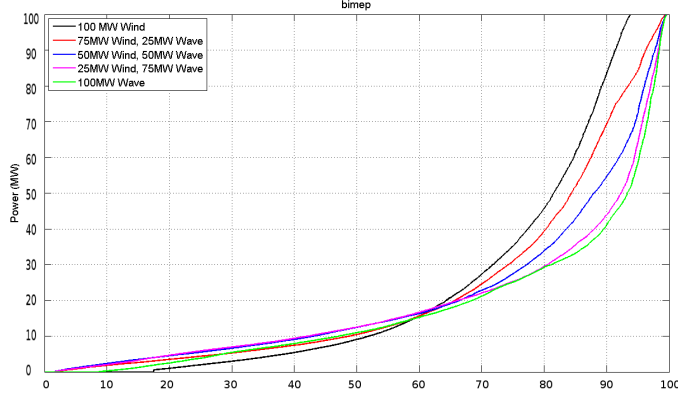


Fig. 5 Non-exceedance power curve at bimep

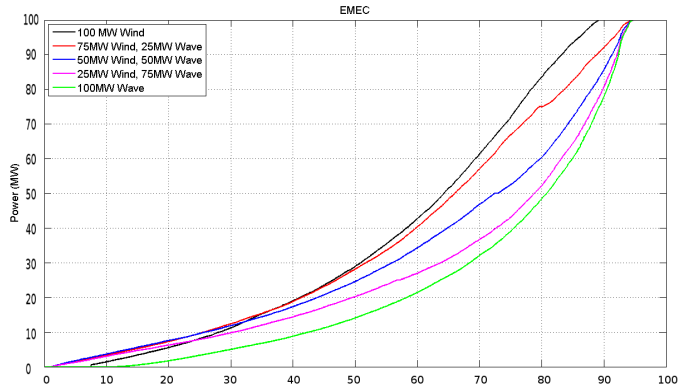


Fig. 6 Non-exceedance power curve at EMEC

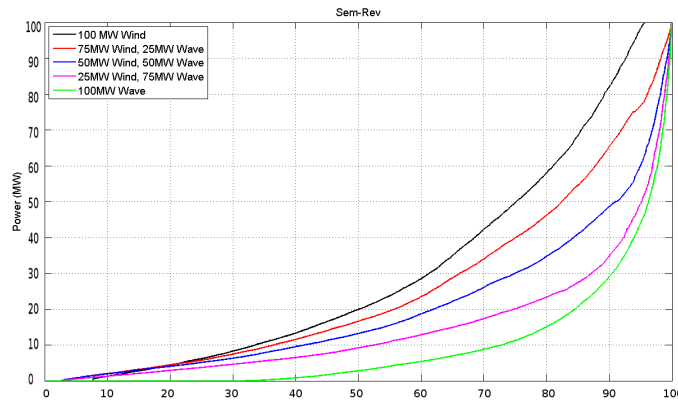


Fig. 7 Non-exceedance power curve at SEM-REV

At SEM-REV, the lower wave power resource combined with the first generation of WECs leads to a poor power distribution for a 100% wave scenario. This is mainly explained by the proportion of small waves (approximately 50% of the waves have a height $H_s < 1\text{m}$ for the 15 month sample). Consequently, wave power is outweighed by wind power. Once again, it is expected in the future that wave energy could help provide better production characteristics, but in a lower proportion than the two previous cases.

C. Power variability

1) Mid-term variability

Mid-term variability refers here to variability at the scale of 1 to 12 hours. Short term variability (of the order of seconds/minutes) is also an important parameter to consider but has not been included in the scope of this study. Table 5 shows the relative produced power variations (ratio of produced power variations after 1-3-12 hours divided by mean produced power). For bimep, the maximum exploitation of wave energy leads to lower variation within a 1-12 hour window. This is probably due to the swells regularly propagating towards the area. These swells generally occur for a duration of half a day to a few days, thus the associated energy level evolves more slowly than the energy associated with wind and wind-induced waves. We can also remark from Table 4 that the available wind resource at bimep fluctuates quite significantly, with the wind velocity standard deviation being the highest of the three sites. This advocates a lower use of wind energy if the power variability is sought to be minimized.

TABLE 5 PERCENTAGE OF OCCURRENCES WHEN THE POWER RELATIVE VARIATION $[(\text{PRODUCED POWER}_{T+\text{TIME HORIZON}} - \text{PRODUCED POWER}_T) / \text{MEAN POWER}]$ IS HIGHER THAN 20%

Time horizon (hr)	Scenarios (MW of wind energy / MW of wave energy)				
	100/0	75/25	50/50	25/75	0/100
bimep					
1	26%	22%	16%	9%	4%
3	48%	44%	38%	26%	15%
12	65%	63%	58%	53%	48%
EMEC					
1	8%	6%	8%	14%	23%
3	33%	28%	27%	28%	35%
12	63%	59%	56%	51%	52%
SEM-REV					
1	12%	11%	9%	10%	17%
3	41%	39%	39%	37%	40%
12	70%	69%	66%	61%	48%

* Shaded cells highlight the scenarios that offer minimum variability

At EMEC, the rate of variability is different if we consider very short time frame (1 to 3 hours) or a longer time horizon (12 hours). Within the first few hours, it appears that more consistent power is obtained from a mix with a significant share of wind energy. Due to the strong wind resource, the occurrence of varying wind seas combined with independent swell seas could explain the relatively high level of variability for 100% wave for a 1 hour window. If we consider a 12 hour time horizon, including wave becomes more preferable as it better captures the slower evolution of high energy swell events.

At SEM-REV, the case is similar to that at EMEC due to the significant wind regime at the site. By introducing an equal mix of 50 MW of both wind and wave energy, 91% of the time the relative hourly variability (power produced difference between 2 hours divided by mean produced power) will stay within 20%. When looking for fewer power variations at longer time horizons (3 to 6 hours), there is also an incentive to have more wave energy in the mix for the same reasons as explained above.

2) Diurnal pattern

Generally, offshore wind has a uniform diurnal pattern if we compare it to onshore wind, however this might not be true as we are closer to the coastline (the effects of the coast might extend up to 30km offshore) where the presence of the land can induce some daily variations such as thermal breezes.

Wave energy is virtually independent of day hours. Oceanic swells propagating towards the coast are independent of the time in the day when they reach the coast. Wind seas can be generated locally at certain hours of the day, but this would be associated with low energetic seas. Hence it can be said that the overall wave energy is quasi-independent of day hour. Fig. 8 highlights the average hourly outputs for the different scenarios for the 2 years of data at bimep. We can see that the 100% wind case presents slight variations throughout the day with higher power produced in the morning from 5:00am to 7:00am. The 100% wave scenario is, as expected, almost independent of the hour in the day.

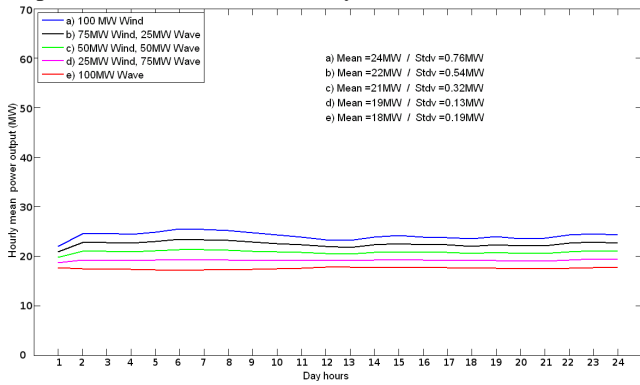


Fig. 8 Hourly variation of power production at bimep

Fig. 9 shows the hourly variations for EMEC. A daily pattern for offshore wind is more obvious, with two peaks - one in the morning around 7-8am, and another one in the evening around 7-8pm. Consequently 2 troughs appear, one at midday and one during the night. This graph also shows slight variations in wave power production with a delay of a few hours from the wind power productions. The two peaks occur at 10-11am and 11-12pm.

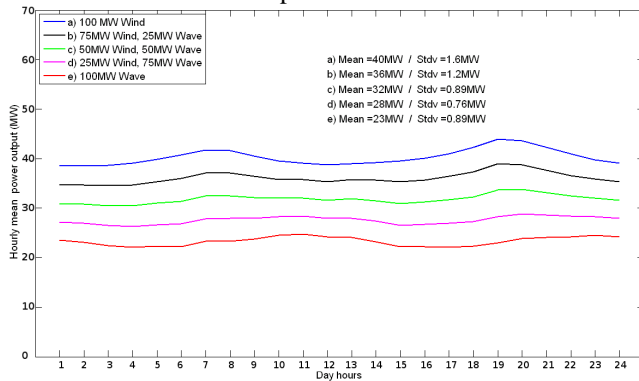


Fig. 9 Hourly variation of power production at EMEC

Fig. 10 shows the situation at SEM-REV, with another distinct pattern. Here the fluctuations are more important for the 100% wave scenario with peaks at 6-7am and 6-7pm. This

could be explained by a very specifically-orientated wind blowing early in the morning and creating wind seas around 6am, then changing direction to reform in the afternoon to create other conditions favourable for the formation of a wind sea. Here the wind power doesn't present as much fluctuation. As such, adding wave power doesn't help in decreasing the hourly variation, but on the other hand, it could help if power demand matched the peak hours of wave power production.

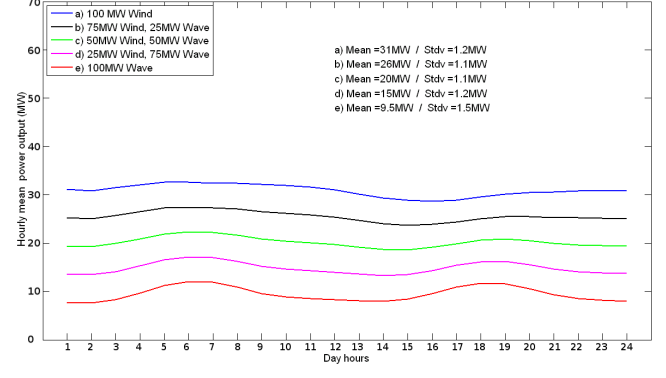


Fig. 10 Hourly variation of power production at SEM-REV

3) Monthly Variation

Finally, Fig. 11 presents the monthly mean power produced according to the different scenarios. At bimep where the wave energy resource is high, the mean monthly power produced when introducing WECs in the energy mix is of the same order for approximately half of the year, and mix tends to be more favourable to a high percentage of wind during the winter months. For the two other sites, and especially at SEM-REV, the mean monthly power production is always negatively affected when wave energy is introduced.

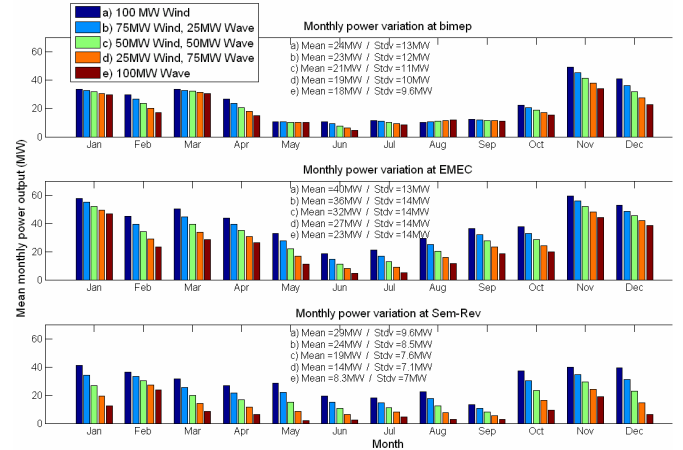


Fig. 11 Monthly mean power for combined scenarios

IV. UK CASE STUDY – MEETING DEMAND

There are two important factors to consider when analysing relationships between output from renewable generators and consumer demand. The first is whether there is general correlation in time between the two time series. 'Intermittency' is frequently cited as a disadvantage of increasing penetrations of renewable energy, particularly wind power, on an electricity network, as it necessitates complex

operational strategies and alternative ‘standby’ generators to maintain supply – both of which can be costly. A consistently good match in time between generation and demand could reduce these requirements.

The second consideration is that production is clearly most critical when the system is experiencing peak consumer demand [14]. It is at these hours when a higher output from renewable generators would be most beneficial to the system.

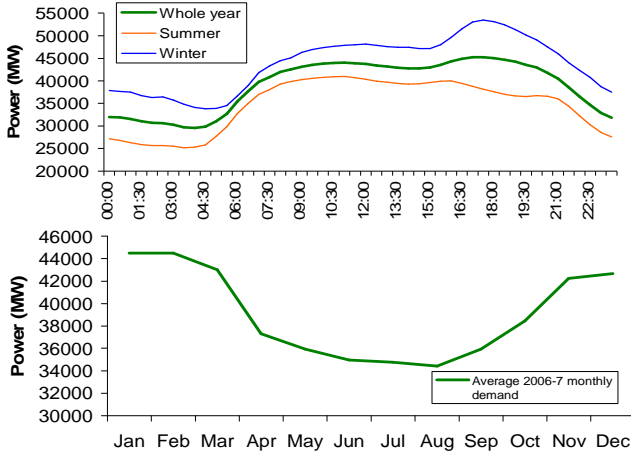


Fig. 12 UK diurnal and annual aggregate demand patterns 2006-07

The half-hourly daily and average monthly demand patterns for the UK are shown in Fig. 12 for the two years 2006-2007 [15]. Comparing the diurnal demand with the diurnal wind power variation at EMEC in Fig. 9 shows that the peaks in power at 07.00 and 19.00 broadly coincide with the morning and evening demand peaks. The midday and midnight ‘troughs’ in power are also fairly coincident with drops in demand. The relatively small variations in wave power shown in Fig. 9 qualitatively appear to bear little relation to demand. The established time-lag in the maximum correlations between wind and wave resources reduces correlation between the resources in any given hour, and thus further strengthens the ability of a combined platform to match demand patterns at peak levels; this is confirmed by the offset in diurnal wind and wave production seen in Fig. 9. This would have beneficial effects in terms of assured revenue and, from a larger-scale, longer-term perspective, might allow a higher capacity value to be assigned to such generators.

The most critical hours of demand occur, fairly obviously, in winter. As shown in Fig. 11 the highest wind and wave power outputs at EMEC also both occur in winter, and so on an average basis, demand and power would seem to be related. On an hour-by-hour basis, however, the relationship may not be so strong. Certain types of circulation pattern, such as when a high pressure is located above the country in winter, known as a ‘blocking anticyclone’, can cause a static period of very cold weather - and hence high demand. These events tend to be associated with strongly negative phases of the North Atlantic Oscillation (NAO). Typically, they result in very low wind speeds over the country. This type of event is likely to have been the cause of the patterns discussed in [16], where it is shown that in the winter of 2007-2008, the capacity factor

of transmission-connected wind farms decreased away from the winter average for times when demand was greater than 90% of the peak demand.

During periods of negative NAO, both wave heights and peak periods in north-western Europe tend to be below average [17][18]. However, because a proportion of the wave energy in these regions is driven by swell associated with distant weather systems, the output from wave power devices located in these areas may not decrease as significantly as that from wind turbines. It is postulated here that WECs might be able to make up some of the shortfall in wind power. A comparison of UK aggregate demand and power production at the EMEC site using data for a 2-year period for various combinations of wind and wave power devices is thus presented. It attempts to establish whether combining different technologies over this period would provide a better match to demand patterns than offshore wind alone, and if further analysis with longer time series is merited.

A. Methodology

In order to quantify the ‘matching’ between demand patterns and power production, a similar method to that used in [1] has been applied. Half-hourly values of aggregate UK demand for Jan 2006 – Dec 2007 [15] have been averaged to an hourly time series and normalised by calculating each hourly value as a percentage of the peak demand during the period of analysis. (This peak occurred in mid-December 2007, coinciding with one of the winter spells described in [16].) The power production is taken from section III for 100MW hypothetical combined technology MRE platform scenarios at the EMEC site.

Those hours where demand as a percentage of peak and the capacity factor are similar (within $\pm 5\%$) are nominally termed ‘best-case’, i.e. relative demand levels match relative production levels. The hours when demand is high as a percentage of peak demand ($>85\%$) and capacity factor is low ($<15\%$) are deemed ‘worst-case’ hours. The numbers of worst-case and best-case hours have been calculated for each scenario of wind-wave combinations.

In order to examine the relationship further, demand (as a percentage of peak) has been classified into 10% bands, and the average capacity factor calculated for each generation scenario at each of the levels of demand. To show more detail for the critical hours, where demand is greater than 90% of peak, the frequency distribution of capacity factors has been calculated for each generation scenario. Finally, an analysis of the highest 20% of demand is presented, by increasing the demand level in increments of 1% and calculating the average capacity factor for all hours with demand greater than this point. This highlights the different activity in the hours of greatest demand for each different generation scenario.

B. Results

Fig. 13 shows that going from a case of 100% wind to a mix of 75% wind and 25% wave gives a small reduction in the percentage of hours with high relative demand and low capacity factor, but a larger increase of about 1% in those

hours with ‘matching’ relative demand and capacity factor. An increase in the contribution of wave power at the site to 50% reduces the worst-case hours very slightly, but there is a correspondingly slight increase in the best-case matching hours compared with wind alone. At a ratio of 25% wind/75% wave and for the 100% wave scenario, there is both a reduction in the best-case hours, and a small increase in worst-case hours, suggesting no advantage from this perspective.

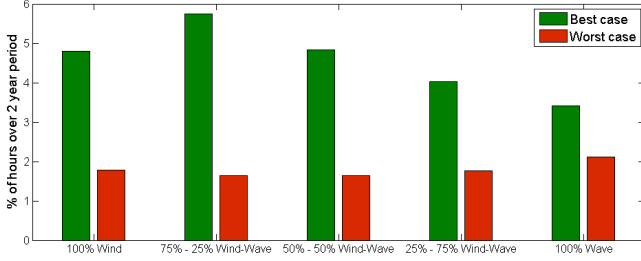


Fig. 13 Numbers of best and worst-case hours for each scenario of wind-wave combination using a Pelamis device power matrix

Fig. 14 presents the average capacity factor for the five combined generation scenarios at differing levels of demand, calculated as a percentage of peak and binned into 10% bands. For all the scenarios, there is a largely positive trend, showing the average capacity factor increasing with demand. It is clear that the average capacity factor is a maximum for all scenarios when demand is 80-90% of peak, but it is difficult to discern any advantage for a particular combination.

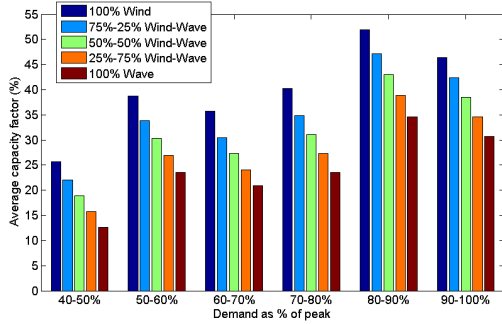


Fig. 14 Capacity factor for each generation scenario for 10% ‘bins’ of demand

The frequency distributions of capacity factors shown in Fig. 15 for demand >90% of peak demonstrate different results, depending on the combination of technologies. For 100% wind power, there are relatively high frequencies of zero and maximum power, whereas these two extremes are of much lower frequency in the 100% wave scenario, with a fairly high frequency of 10-30% capacity factors. A flatter distribution over all capacity factors is present in the combined wind-wave scenarios. Again, however, it is difficult to identify one scenario as particularly advantageous for these hours, but they do very clearly offer different outcomes.

Fig. 16 is an adaptation from [16] which shows, in blue, the average capacity factors for the 5 generation scenarios (on the y-axis) where demand is greater than X% of peak, with X shown on the x-axis. The percentage of the total number of hours over which the average capacity factors at each demand level were calculated is shown by the green line. Capacity factor clearly falls as demand increases from 80-100% of peak, and as with [16], the wind power capacity factor drops

dramatically at the point of absolute peak demand – this was identified as being during a period of anti-cyclonic activity over the UK.

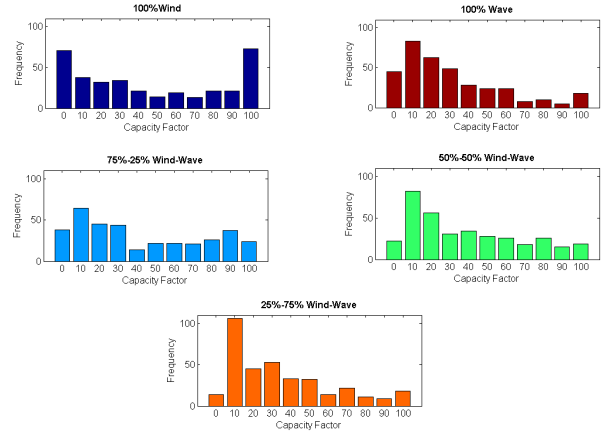


Fig. 15 Capacity factor frequency distributions for each generation scenario when demand is >90% of peak.

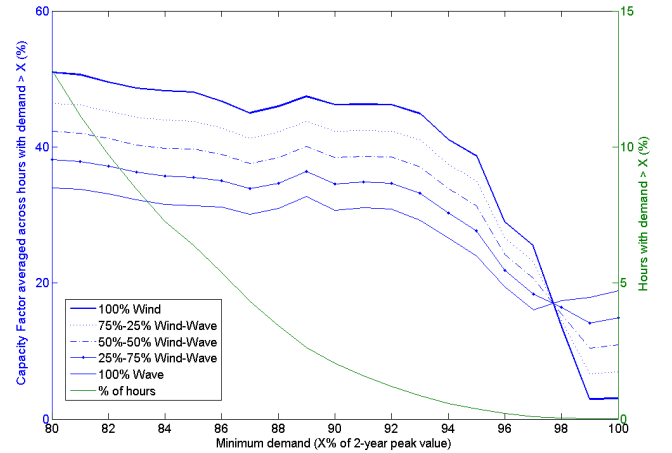


Fig. 16 Adapted from [16] showing the average capacity factors for the MRE scenarios where demand is above X% of peak

However, the capacity factor for the 100% wave scenario begins to recover slightly at the >97% level. Any scenarios which include wave generation do not drop as steeply as the 100% wind scenario, potentially indicating that in these situations, wave devices may compensate to some degree for the loss of wind power. It is important to note that there were only 11 hours in total with a demand greater than 98% of peak, and thus the average capacity factors here are calculated over a relatively small number of hours. There is a physically-driven basis for believing that it will be repeated in other instances of these types of high-demand events, but analysis of longer time series is necessary.

V. CONCLUSIONS

The work in section II of the paper showed that wave and wind power show medium to high correlation at each of the three sites, with evidence that the wave time series lags the wind by between 1 and 5 hours. The bi-variate distribution for wave and wind power is an interesting output since it shows the layout distribution of the power levels and their correlation. A large distribution implies a low overall correlation, which is

the case at SEM-REV. Narrow distributions indicate high correlation between wind and wave power, as has been shown for bimep and EMEC test sites. More work is required to establish any patterns in correlation that may depend on seasonality, but longer data sets will be considered in order to account for inter-annual variability.

Section III of the paper focused on the implications of the resource correlations for device output at the three test sites using hypothetical combinations of existing wind and wave energy devices. The direct comparison of wind turbine and WEC power outputs is biased by the differing levels of development of both technologies, so introducing wave power into the generation scenarios significantly reduces the power.

The non-exceedence curves highlight the distinction between the three sites, and how the ideal mix of wind and wave power would vary by site. The 1-to-12 hour variability is also seen to vary by site, due to their differing resource characteristics, but generally, the addition of wave power to the mix is beneficial, particularly over longer time horizons. The diurnal variability of wind and wave power are quite different, with wind power typically showing some evidence of morning and evening peaks at each site. Wave power tends to be quasi-independent of the time of day (except for SEM-REV – where the variation of the wave height is seemingly affected by the tidal regime), and thus adding wave generation to a site could provide more constant production.

In terms of monthly variation, wind power, and to a lesser degree, wave power, tend to peak in winter and fall in summer, with the pattern being particularly strong in the UK. This matches a typical UK demand pattern, with its peak in winter and a significant drop in summer months. The pattern is also present in the Spanish and French sites, but the tendency for the monthly demand to follow a similar trend is not so strong, with, for example, regions in the south of Spain having their demand peak in summer to meet space cooling requirements.

The analysis of diurnal and monthly variability provided a basis for the hypothesis presented in section IV, which was that combined MRE platforms utilising both wind and wave power would offer a better match to consumer demand than a development employing wind power alone. This was tested using conditions at the EMEC site in Scotland. Consumer demand was modelled using UK total demand, normalised by the peak demand to give relative hourly values over a 2 year period. The results show that a combination employing a 75%-25% wind-wave ratio gives a slightly reduced number of hours with high relative demand and low capacity factor, and a more significant increase in the number of hours where the relative demand and relative production levels are similar.

Examining the hours of peak demand in detail shows that during the cold spells where wind generation reduces, wave power does not reduce so significantly. It is difficult to apply statistical rigour to this analysis, based as it is on output for one site for a small number of critical hours, but it indicates that with provision of longer time series, further analysis using multiple European-wide sites and power characteristics from some of the preliminary combined platform designs developed from the MARINA Platform project would be of interest.

ACKNOWLEDGMENT

The authors would like to acknowledge support from the MARINA Platform partners and the EU FP7 (Grant agreement number: 241402). The following are gratefully acknowledged for provision of data and data-support: EMEC, SEM-REV, EVE, AZTI-Tecnalia, Sam Hawkins (University of Edinburgh), Charlotte Hassager and Xiaoli Guo Larsén (Risø), MétéoGalicie, Meteodyn.

REFERENCES

- [1] (2011) Marina-Platform Website. [Online]. Available: <http://www.marina-platform.info/>
- [2] Bierbooms, W. (ed.) "DOWEC (Dutch Offshore Wind Energy Converter project) wind and wave conditions report". DOWEC 47 rev. 2, W. Bierbooms (ed.). Delft University of Technology.
- [3] EquiMar (2011). "Wave and tidal resource characterization". Available: <http://www.equimar.org/equimar-project-deliverables.html>
- [4] The WAMDI Group (1988). The WAM model – "A third generation ocean wave prediction model". *Jour. of Phys. Oceanogr.*, 18:1775-1810.
- [5] (2011) Previmer Website [Online]. Available: <http://www.previmer.org>
- [6] Michalakes, J., S. Chen, J. Dudhia, L. Hart, J. Klemp, J. Middlecoff, and W. Skamarock: "Development of a Next Generation Regional Weather Research and Forecast Model. Developments in Teracomputing", *Proceedings of the Ninth ECMWF Workshop on the Use of High Performance Computing in Meteorology*. Eds. Walter Zwiefelhofer and Norbert Kreitz. World Scientific, Singapore, 2001, pp. 269-27.
- [7] L. Ferrer, P. Liria, R. Bolanos, C. Balseiro, D. Gonzalez-Marco, M. Gonzalez, A. Fontan, J. Mader and C. Hernandez. "Reliability of coupled meteorological and wave models to estimate wave energy resource in the Bay of Biscay". *Proceedings of the 3rd International Conference on Ocean Energy*, ICOE Bilbao 2010.
- [8] R. Nerzic, M. Prevosto. "Modelling of Wind and Wave Joint Occurrence Probability and Persistence Duration from Satellite Observation Data", *Proceedings of the 10th IOPEC*, ISOPE 2000.
- [9] F. Fusco, G. Nolan, J. Ringwood. "Variability reduction through optimal combination of wind/wave resources – An Irish case study." *Energy* 35, 2010, pp. 314-325.
- [10] Vestas Wind Systems A/S. 2004. V90-3.0 MW Product Brochure. Rinköping: Vestas.
- [11] G.J. Dalton, R. Alcorn, T. Lewis, "Case study feasibility analysis of the Pelamis wave energy convertor in Ireland, Portugal and North America", *Renewable Energy*, vol. 35, 2010, pp.443-465.
- [12] A. Babarit, J. Hals, A. Kurniawan, T. Moan, J.Krokstad. "Power absorption measures and comparisons of selected wave energy converters". *Proceedings of the ASME 2011 30th International Conference on Ocean, Offshore and Arctic Engineering*, OMAE 2011, Rotterdam.
- [13] E. Friis-Madsen, Personal Correspondence, 2011.
- [14] G. Sinden, "Characteristics of the UK wind resource: Long-term patterns and relationship to electricity demand", *Energy Policy*, vol. 35, pp. 112-127, Dec. 2005.
- [15] (2011) UK National Grid: Metered half-hourly electricity demand [Online]. Available: <http://www.nationalgrid.com/uk/Electricity/Data/Demand+Data/>
- [16] A. Keane, M. Milligan, C.J. Dent, B. Hasche, C. D'Annunzio, K. Dragoon, H. Holttinen, N. Samaan, L. Söder, M. O'Malley, "Capacity value of wind power", *IEEE Transactions on Power Systems*, vol. 25, Sep. 2010.
- [17] G. Dodet, X. Bertin, R. Taborda, "Wave climate variability in the North-East Atlantic Ocean over the last six decades", *Ocean Modelling*, vol. 31, 2010, pp. 120-131.
- [18] D. K. Woolf, P.G. Challenor, P.D. Cotton, "Variability and predictability of the North Atlantic wave climate", *Journal of Geophysical Research*, vol. 107, 2002.
- [19] T. Boehme, J. Taylor, A. R. Wallace, J. Bialek, "Matching Renewable Electricity Generation With Demand". Edinburgh, U.K.: Scottish Executive, Feb. 2006.